Theses and Dissertations | 1. Thesis and Dissertation Collection, all items

1994-12

Design of a superelastic alloy actuator for a minimally invasive surgical manipulator

Parkhurst, William T.

Monterey, California. Naval Postgraduate School

NAVAL POSTGRADUATE SCHOOL
MONTEREY, CALIFORNIA

THESIS

DESIGN OF A SUPERELASTIC ALLOY
ACTUATOR FOR A MINIMALLY INVASIVE
SURGICAL MANIPULATOR

by

William T. Parkhurst II

December, 1994

Thesis Advisor: Ranjan Mukherjee

19950517 065

DTIC QUALITY INSPECTED 5

REPORT DOCUMENTATION PAGE

Form Approved OMB No. 0704-0188

1. AGENCY USE ONLY *(Leave blank)*	2. REPORT DATE December 1994	3. REPORT TYPE AND DATES COVERED Master's Thesis

4. TITLE AND SUBTITLE DESIGN OF A SUPERELASTIC ALLOY ACTUATOR FOR A MINIMALLY INVASIVE SURGICAL MANIPULATOR	5. FUNDING NUMBERS

6. AUTHOR(S) William T. Parkhurst II

7. PERFORMING ORGANIZATION NAME(S) AND ADDRESS(ES) Naval Postgraduate School Monterey CA 93943-5000	8. PERFORMING ORGANIZATION REPORT NUMBER

9. SPONSORING/MONITORING AGENCY NAME(S) AND ADDRESS(ES)	10. SPONSORING/MONITORING AGENCY REPORT NUMBER

11. SUPPLEMENTARY NOTES The views expressed in this thesis are those of the author and do not reflect the official policy or position of the Department of Defense or the U.S. Government.

12a. DISTRIBUTION/AVAILABILITY STATEMENT Approved for public release; distribution is unlimited.	12b. DISTRIBUTION CODE

13. ABSTRACT *(maximum 200 words)*

The purpose of this research is to investigate and develop actuators for a minimally invasive surgical manipulator using a Superelastic Alloy (SEA) as the active element. The actuator, an SEA tube, is designed to take advantage of the transformational psuedoelasticity property found in near equiatomic Ni-Ti alloys. The characteristics of SEA as an actuator are illustrated, with an emphasis on the concept of temperature dependency of stress and strain. This concept is used to develop a theory to control the motion of the individual active elements. With an elevation of temperature comes a change in the resistance that is repeatable but not completely explained to date. This change provides an ideal way to measure temperature for feedback by indirectly measuring resistance. Our design will integrate a series of actuators and a structural skeleton into a manipulator that is intrinsically simple, capable of exerting large forces, compact in size and extremely dexterous.

14. SUBJECT TERMS Superelastic, Actuator, Manipulator	15. NUMBER OF PAGES 48
	16. PRICE CODE

17. SECURITY CLASSIFICATION OF REPORT Unclassified	18. SECURITY CLASSIFICATION OF THIS PAGE Unclassified	19. SECURITY CLASSIFICATION OF ABSTRACT Unclassified	20. LIMITATION OF ABSTRACT UL

NSN 7540-01-280-5500

Standard Form 298 (Rev. 2-89)
Prescribed by ANSI Std. 239-18 298-102

Approved for public release; distribution is unlimited.

DESIGN OF A SUPERELASTIC ALLOY ACTUATOR FOR A MINIMALLY
INVASIVE SURGICAL MANIPULATOR

by

William T. Parkhurst II
Lieutenant, United States Navy
B.S., United States Naval Academy, 1989

Submitted in partial fulfillment
of the requirements for the degree of

MASTER OF SCIENCE IN MECHANICAL ENGINEERING

from the

NAVAL POSTGRADUATE SCHOOL
December 1994

Author:

William T. Parkhurst II

Approved by:

Ranjan Mukherjee, Thesis Advisor

Matthew D. Kelleher, Chairman
Department of Mechanical Engineering

iii

Accession For	
NTIS GRA&I	☑
DTIC TAB	☐
Unannounced	☐
Justification	

By
Distribution/

Availability Codes	
Dist	Avail and/or Special
A-1	

ABSTRACT

The purpose of this research is to investigate and develop actuators for a minimally invasive surgical manipulator using a Superelastic Alloy (SEA) as the active element. The actuator, an SEA tube, is designed to take advantage of the transformational psuedoelasticity property found in near equiatomic Ni-Ti alloys. The characteristics of SEA as an actuator are illustrated, with an emphasis on the concept of temperature dependency of stress and strain. This concept is used to develop a theory to control the motion of the individual active elements. With an elevation of temperature comes a change in the resistance that is repeatable but not completely explained to date. This change provides an ideal way to measure temperature for feedback by indirectly measuring resistance. Our design will integrate a series of actuators and a structural skeleton into a manipulator that is intrinsically simple, capable of exerting large forces, compact in size and extremely dexterous.

iv

TABLE OF CONTENTS

I. INTRODUCTION

Several actuators for miniature robots with applications such as minimally invasive surgery have been researched and are currently being explored [Ref. 1, 2, 3, 5, 7, 8, 9, 10, 11, 12, 14, 16, 17]. Many actuators being developed are made of Shape Memory Alloys (SMA) which operate on the principle of transforming thermal energy, induced most commonly through Joule heating, into mechanical work [Ref. 4, 5]. Shape Memory Alloys are Nickel-Titanium (Ni-Ti) binary alloys, whose Martensitic finish temperature (M_f) and Austenitic finish temperature (A_f) depend on the atomic percentages of the two elements. The most common SMA have an A_f of around 40°C to 60°C above room temperature. A special class of SMA's are the Superelastic Alloys (SEA) that have near equiatomic percentages of Nickel and Titanium. Superelastic Alloys typically have an A_f below room temperature. Though SEA's are a special class of SMA's, in this thesis we will refer to SMA's as those Ni-Ti binary alloys that do not exhibit superelastic behavior.

While SMA actuators have a number of advantages over conventional actuators, they have two major drawbacks. To achieve full shape memory effect, the SMA actuator must be heated to above A_f and subsequently cooled to below M_f. The temperature interval between A_f and M_f is typically 20°C to 30°C, and even with forced convection, the time required for cooling could be too long for the actuator to have a modest bandwith [Ref. 6]. When SMA actuators are used in the wire form, only a small range of motion is available. This problem becomes acute in small mechanisms, such as miniature robots, where mechanical amplification of motion is difficult. Researchers in the past have tried using SMA coil springs to overcome this displacement problem [Ref. 7]. SMA coil springs can provide larger displacements but only at the expense of the actuating force.

We propose to use an SEA tube for an actuator to overcome the drawbacks of conventional SMA actuators. The problem associated with the cooling of the SMA actuator is not encountered with the SEA actuator for reasons to be explained later in this thesis. SEA's are capable of withstanding higher stresses than conventional Shape

Memory Alloy, and therefore an SEA tube can provide large displacements along with moderately high actuating forces. An SEA tube is a better choice for an actuator than an SEA solid rod. Both have comparable stiffness as their area moments of inertia are similar, but the SEA tube has a significantly lower cross-sectional area and therefore, a much higher resistance. This makes electrical heating a more feasible option.

Minimally invasive surgical procedures have become very popular in the past few years. They are cost effective, less painful to the patient undergoing surgery and are performed on an outpatient basis, compared to conventional surgical procedures which can result in weeks of hospitalization. However, due to the lack of advanced surgical instrumentation, operating time is significantly high for minimally invasive procedures. The purpose of this research is to design and begin the development of an SEA tube actuator to be used in an externally controllable and flexible robotic manipulator. This manipulator will be able to pass through a standard trocar and maneuver dexterously within the torso of a patient. The flexible robotic arm will resemble a controllable snake and will be capable of following a serpentine path of tight radii. The surgeon will connect an end-effector of choice, a scissor or stapler for example, to the manipulator for use in surgical procedures.

The specific requirements for the manipulator are: (a) the outside diameter must be no greater than 10 mm, (b) it must be flexible and capable of dexterous manipulation, (c) it should be structurally strong enough to generate forces required for normal surgical procedures like cutting and stapling, and (d) there must be a hollow annular space along its' length for the passage of optical fibers or control cables, etc. depending upon the surgical procedure necessary. For example, if the robotic manipulator is to be used as a laparoscope for visual examination of internal organs, a camera will be mounted on the end of the manipulator and fiber optic cables will pass through the annular hollow space. If an incision is necessary, the end-effector would be a pair of scissors. Cables passing through the hollow annular space of the manipulator would control the scissors' cutting action. Refer to Figure 1 for a schematic diagram.

2

This thesis is organized in the following order. Chapter II is a literature survey of the past research and development of actuators for miniature robots. Chapter III provides an introduction to Shape Memory and Superelastic Alloys, describes the advantages of Superelastic Alloys over Shape Memory Alloys, explains the fatigue in SEA over a large number of cycles and illustrates the resistance-temperature characteristics of SEA tubes over a temperature range of interest to us. Chapter IV introduces the concept behind the SEA tube actuator and emphasizes the advantages of the SEA tube actuator. The design of the SEA actuator and its integration into the surgical manipulator is also discussed in this chapter. Chapter V summarizes the gains of this research and recommendations for further study.

The motion of the flexible robot arm will be controlled by commands given from the keyboard of the control computer. In future, a man-machine interface will be built so that the flexible robot arm can be controlled by voice commands of the surgeon.

Control Computer

electrical cables driving the actuators are connected to the control computer

inside the human torso

Tube for blowing air into the arm for cooling the actuators

standard size trocar

Flexible robot arm with a hollow interior

simple mechanical device to be used by the surgeon for end-effector control.

mount for end-effector

End-effector to be connected to the end of the flexible robot arm. An end-effector like a pair of scissors, or a gripper will be controlled by cables that will pass through the hollow space within the flexible robot arm to a device that will be controlled by the surgeon.
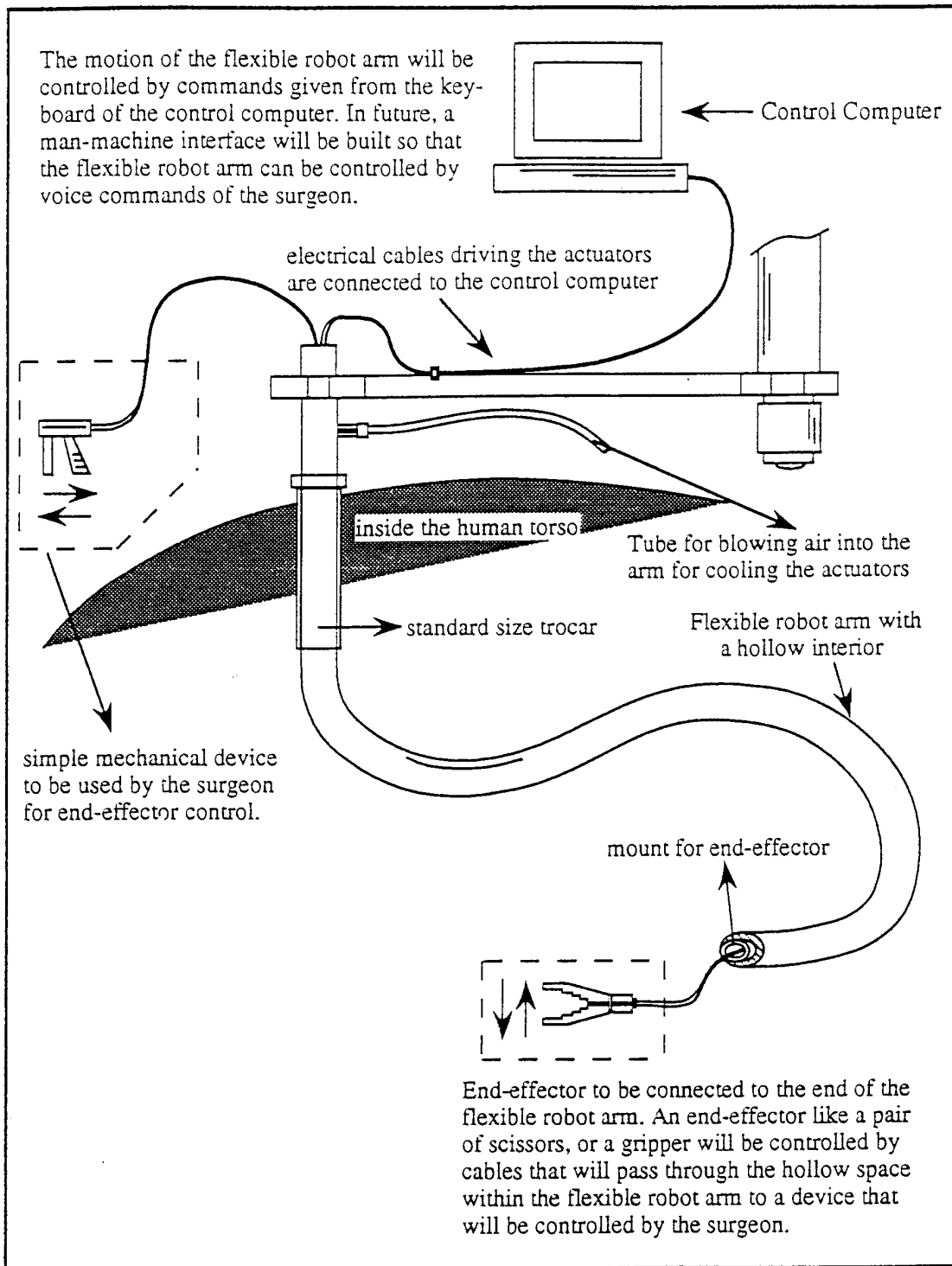
Figure 1. A conceptual minimally invasive surgical manipulator.

II. LITERATURE SURVEY

A number of researchers have addressed the problems of using SMA actuators in robotics and the design of miniature devices for minimally invasive surgical procedures. In this section, some of the better known research pertinent to our work is reviewed.

The actuators researched by Bergamasco, et al. [Ref. 1, 8] were based on SMA helical springs. They were compact enough to be easily incorporated into the phalangeal structure of a robotic finger, thus eliminating the complex routing of cables and tendons used for transmitting motion from conventional actuators. A simple SMA wire can exert a large reversion force, but as compared to an SMA spring, the deformation is considerably small. Bergamasco, et al. reached an acceptable compromise between force and deformation by designing the spring to have a very small diameter. For our flexible robotic manipulator, the force requirements are much higher than those that can be supported by the SMA active elements in [Ref. 1, 8]. This is due to the considerable amount of structural rigidity needed by the manipulator to support the end-effector as it applies a force.

A Micro Active Catheter (MAC) with embedded SMA actuating elements was developed and tested by Fukuda, et al. [Ref. 9]. It is designed to navigate smoothly through body cavities and soft tissues. The MAC is a flexible lumina catheter (designed in three diameters -1.33 mm, 1.66 mm, or 2.0 mm) that has three active bending units on the tip which are connected by elastic joints. Three SMA wires are embedded in the lumina 120° around the centerline of each bending unit which gives the MAC two degrees of freedom. This catheter is more suitable as a probe for soft tissues due to its lack of rigidity.

An active catheter tip actuated by SMA elements was designed for medical intercavity intervention by Dario, et al. [Ref. 10]. The purpose of their research was to study the ability of the active catheter tip to generate large displacement and moderately large forces at low frequency. A miniature device was fabricated using a commercial 6f catheter (approximately 2.4 mm diameter). The actuation was provided by SMA wires

which were annealed in a "U" shape at 570°C. Liquid flowing through the walls of the catheter was the medium used to heat and cool the SMA wires. Catheter motion was controlled through feedback signals from the fiber-optic sensors embedded in the catheter. The main drawbacks of the design, which make it unsuitable for our purpose, are only the tip of the catheter is controllable, with just one degree of freedom, and the small forces generated by the SMA active elements. However, the use of fiber-optic sensors to measure the angular displacement of the device may be useful in our future research. The results Dario, et al. achieved, indicated the necessity of further investigation to complete characterization of SMA material in terms of stress-strain-temperature relation, and "limit curves" that allow the working conditions to be accurately defined for total reversibility. Bergamasco, et al. reached a similar conclusion [Ref. 1,8].

A mathematical model of the SMA for designing a micro actuator was developed by Ikuta , et al. [Ref. 11]. They proposed an advanced three phase mathematical model of Shape Memory Alloy useful in the design of SMA micro devices. The model was applied to the coil spring theory to analyze their mechanical and electrical characteristics. Ikuta, et al. suggested that the direction of future research should combine finite element modeling with the SMA model to realize the SMA-CAD for micro devices.

Some basic research for the use of Ti-Ni SMA as a micro actuator was conducted from a crystallographic point of view by Ikuta, et al. [Ref. 12]. The potential of Shape Memory Alloys as micro actuators was discussed by Ikuta [Ref. 13]. The static and dynamic properties of Ti-Ni Shape Memory Alloy wires were analyzed by Kuribayashi [Ref. 3]. The control system for an SMA actuator was synthesized by pulse width modulated (PWM) controllers, and experiments for the position and force control of the actuators were carried out. Kuribayashi also designed and fabricated a Shape Memory Alloy millimeter-sized actuator for driving a rotary joint for a small robot [Ref. 2]. The actuator was of push-pull type and composed of two SMA sheets.

Shape Memory Alloy servo actuators were used for the development of an active endoscope by Ikuta, et al. [Ref. 7]. This research is pertinent to our own, as the

endoscope is similar to the flexible manipulator we intend to develop. Their endoscope was a real size active endoscope consisting of five segments, 40 mm in length and 13 mm in diameter. Each individual segment was externally controlled by antagonistic electric resistance feedback without any position sensors. The SMA wires were connected in parallel mechanically, but in series electrically. The system had a number of advantages due to the use of antagonistic type resistance feedback control. The hysteresis of the SMA actuators was reduced and the overheating of the SMA wires was prevented. We intend to use electric resistance feedback control for our flexible manipulator as well. The main drawbacks of the Ikuta, et al. design include: (a) the structural skeleton lacks strength and droops under its own weight when the SMA actuators are not active, (b) it is limited to one degree of freedom, and (c) it can only be used as a probing device and not as a manipulator due to its lack of structural rigidity. In addition, incorporation of an externally controllable end-effector would require major changes in the design of the endoscope. The endoscope would then require a hollow annular interior to enable the passage of control cables for the end-effector. The purpose behind the development of our flexible manipulator is to provide a surgeon with accessibility to internal organs with minimal invasion. The endoscope designed by Ikuta, et al. must undergo major design changes before it may be used as a flexible manipulator.

A flexible microactuator (FMA) driven by an electro-pneumatic (or electro-hydraulic) system was developed by Suzimori, et al. [Ref. 14]. The FMA has three degrees of freedom: pitch, yaw, and stretch, and these are suitable movements for miniature robotic mechanisms such as robotic fingers, arms and legs. The FMA is constructed of fiber reinforced rubber, quite simple in design, and can replace conventional linkages in miniature robots. Serially connected FMA's can be used as a flexible robotic manipulator; the kinematics and control for such a flexible manipulator is discussed by Suzimori, et al [Ref. 14]. Though the ideas behind their research is novel, it is not beneficial to our research for two major reasons: the available force from the tip of a 10 mm diameter serially linked FMA is too small and their is no viable way to incorporate an

annular space into the manipulator without major design changes and significant loss of structural rigidity.

Shahinpoor proposed the use of ionic polymer gel fibers as actuators [Ref. 15]. In one of his designs, a cylindrical helical compression spring was encapsulated and hermetically sealed in a mixture of ionic polymeric gel fibers and a counter-ionic solution. The second design comprised of a fiber bundle of SMA circumscribed inside a helical compression spring with flat heads. The fibers were electrically heated and subsequently contracted to compress the helical compression spring back and forth. The proposed actuator models are quite novel but the single degree of motion, limited displacement of the SMA fibers and its lack of strength make it unsuitable for our application.

Some recent work on robotic manipulators is quite pertinent to our research. A hyper redundant active endoscope driven by miniature cybernetic linear actuators has been developed by Ikuta, et al. [Ref. 16]. This endoscope is controlled by a master-slave force feedback system with friction control and dither so that the surgeon can feel the reaction forces on the endoscope during surgical operation. Neisius, et al. developed a robotic manipulator capable of endoscopic support of surgical end-effectors and cameras [Ref. 17]. It involves an instrument shaft capable of passing through a trocar, and a multiple degree of freedom endoscopic multi-link structure driven by miniature servo motors with planetary gears. The surgical end-effectors include grippers, scissors, a multifunctional bipolar coagulation forceps and a pneumatically controlled sewing instrument.

III. SUPERELASTIC ALLOY PRELIMINARIES

A. INTRODUCTION TO SUPERELASTIC ALLOYS

A Superelastic Alloy is a specific type of Shape Memory Alloy. For an SMA, the shape memory effect is both thermal and mechanical in nature. The shape memory effect of an SMA is best described with reference to Figure 2. As the specimen is cooled from
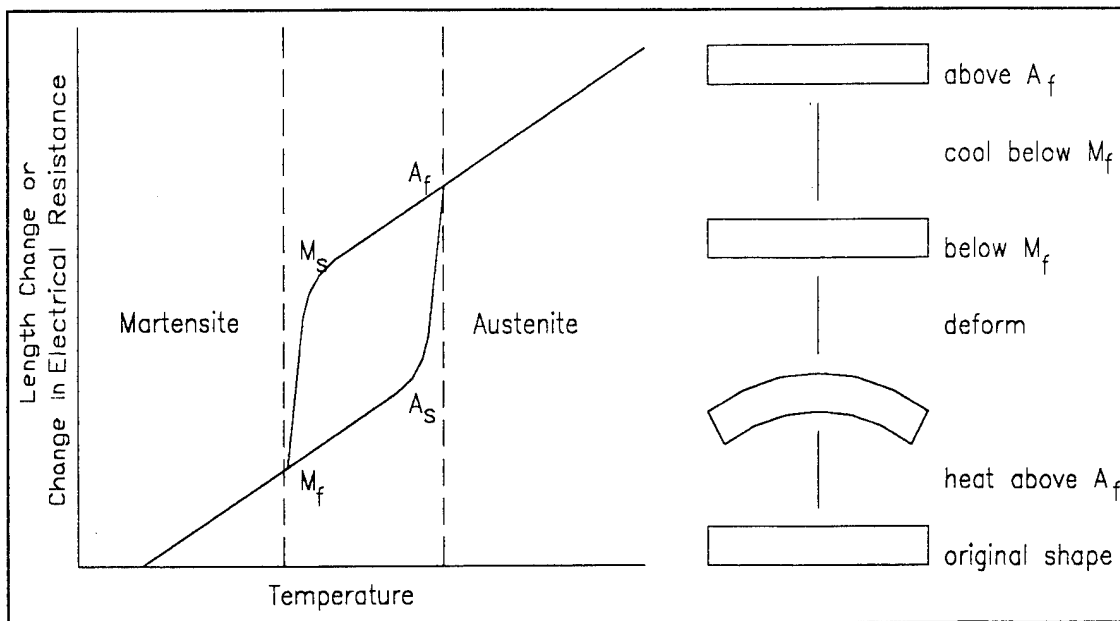

Figure 2. The shape memory effect of SMA illustrated in a theoretical plot of electrical resistance vs. temperature and an example of a specimen.

above A_f to below M_f the shape remains constant. This is due to the phase transformation of austenite into twinned martensite. If the specimen is deformed below M_f, the deformation will remain, the result of the twin boundaries found in martensite migrating under shear, which produces several variants to accommodate the deformation. To induce the full shape memory effect, the specimen is then heated above A_f. The original shape

begins to recover when the specimen reaches A_s as the phase transformation of martensite to austenite commences. When the temperature of the specimen reaches A_f, the phase transformation is completed and the specimen regains its original shape. Upon cooling to below M_f, there is no shape change as the austenite transforms back to the twinned martensite. So in SMA, the phase transformation associated with the shape memory effect are caused by heating and cooling of the specimen. The formation of martensite in SMA is known to be a thermoelastic process. In other words, incremental changes of temperature between M_s and M_f result in corresponding increases and decreases in the growth of the martensite plates [Ref. 18, 19, 20, 21].

In order for an SEA to exhibit superelastic behavior, the alloy must be deformed above A_f but below M_d. The values of all characteristic temperatures of the SEA - Martensite Start and finish temperatures, (M_s and M_f) and Austenite Start and Finish Temperatures (A_s and A_f) - are dependent on the value of M_s. Figure 3 shows graphically the relative positions of these temperatures. The value of M_s is initially determined by the Ni-Ti atomic composition but it can be seriously affected by prolonged exposures to high annealing temperatures. Ni-Ti alloys with compositions of Ni-50.0 at.% Ti have an approximate A_f of 5.0°C and therefore have superelastic properties at and above room temperature. Annealing of the alloy at elevated temperatures tends to raise the value of M_s depending on the time and temperature of annealing [Ref. 4, 21].

The formation of martensite in an SEA is the result of an external stress applied to the specimen, not a temperature change. An increase of the applied stress promotes the growth of martensite while a decrease in stress results in the shrinking of martensite plates [Ref. 20, 21]. This form of martensite, called Stress Induced Martensite (SIM) accommodates the shape change in an SEA. When an SEA specimen is deformed, martensite plates grow from the austenite parent phase when the internal stresses in the specimen equal a critical stress value. The result is the specimen exhibiting a large strain and a constant stress plateau. The plateau is a result of the SIM forming anywhere the stress in the specimen reaches the critical stress. The stress in the specimen will not

increase above the critical stress, known as σ_l or loading stress, as long as SIM can grow to accommodate the strain. The loading stress is limited by the maximum allowable strain, of the order of 8% for most SEA's [Ref. 4, 18, 19, 20].

Figure 4 shows the superelastic shape memory effect. The SEA specimen is deformed at a temperature above A_f but below M_d. The stress in the specimen will increase until it reaches the σ_l necessary for the growth of SIM. As the specimen is
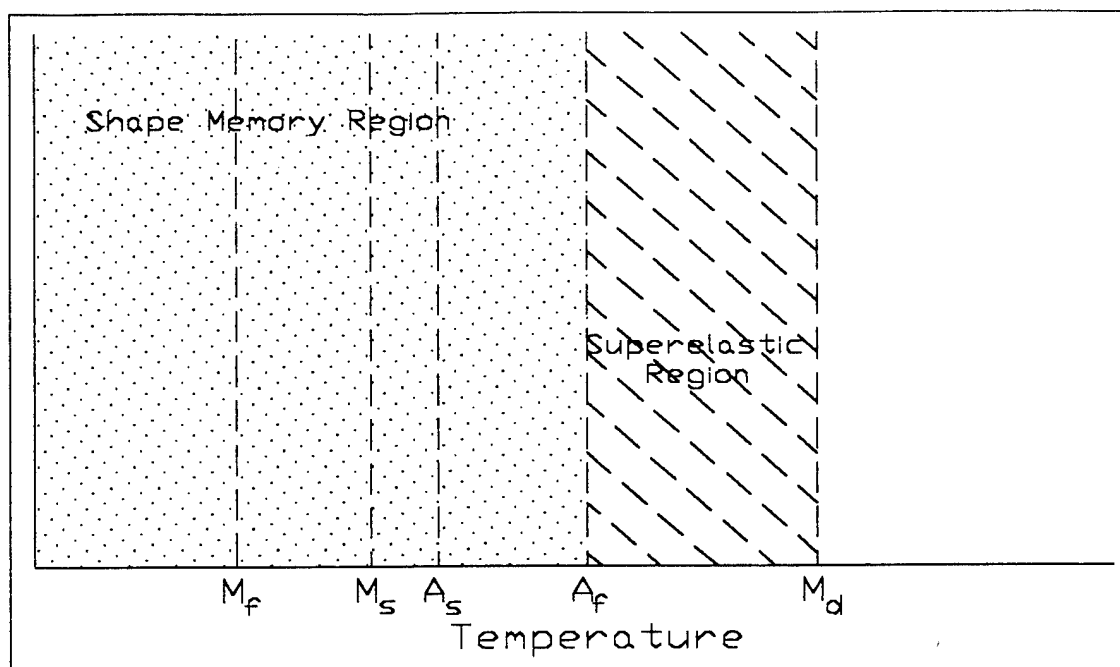

Figure 3. Temperature regions of an SMA and SEA [Ref. 20].

deformed further, the growth of SIM will accommodate the strain and the superelastic stress plateau will be evident till approximately 8.0% strain. If the force required to deform the specimen is reduced, the martensite will begin to disappear and a hysteresis will develop as the internal stress lowers to σ_u, the unloading stress. The resulting martensite to austenite phase transformation drives the specimen to its original

undeformed shape just as in the SMA, only no thermal input is needed. As the stress is reduced to zero, full shape memory is obtained [Ref. 4, 18, 19, 20].

The hysteresis associated with the stress-strain curves of SMA and SEA is associated with martensitic transformation. In both cases, the hysteresis is attributed to the friction between the martensite boundaries. In the SMA, there is a higher friction associated with the twinning of martensite boundaries as they form upon cooling. In the SEA, there is a higher friction associated with the growth of similar boundaries in SIM
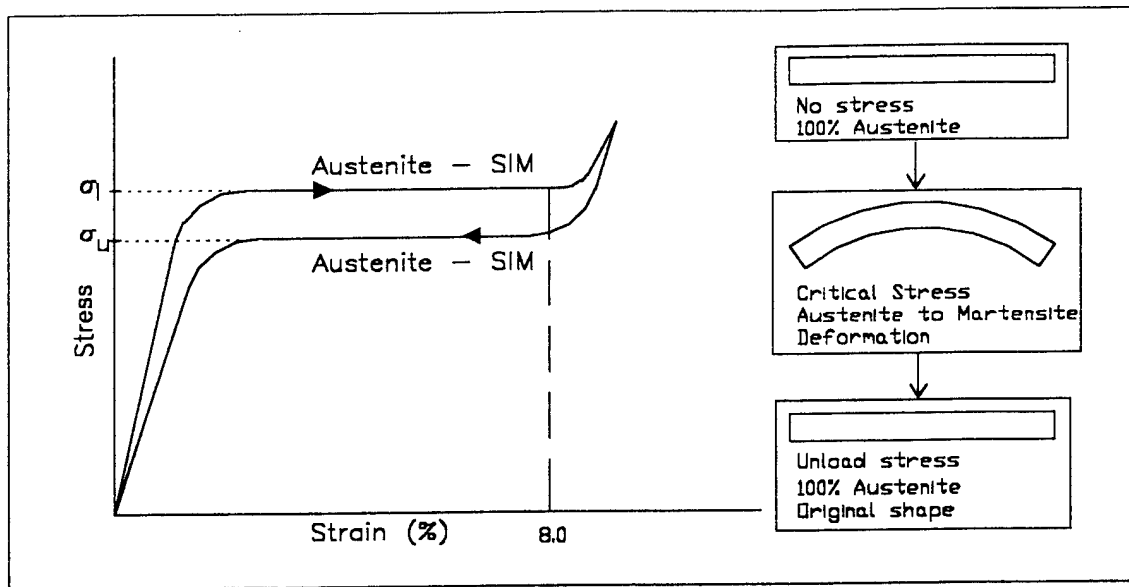

Figure 4. Theoretical stress-strain curve of a Superelastic Alloy and an example of a specimen undergoing deformation and shape memory.

[Ref. 18, 20, 22, 23]. All forms of SMA exhibit this hysteresis to varying degrees.

Superelasticity can only be realized between A_f and M_d. In this temperature range, σ_l required to induce martensite is linearly related to the temperature of the alloy. As the temperature of the SEA increases, the amount of stress needed to create SIM increases. This relation follows the Clausius-Clapeyron equation up to M_d [Ref. 4, 18, 19, 21].

Above this temperature, the σ_1 required to induce martensite is greater than that needed to move dislocations. In other words, above M_d plastic deformation due to slip is easier with the application of stress than creating SIM to accommodate the strain. Stress causes dislocation boundaries to move which results in permanent deformation. Hence, M_d is the highest temperature at which SIM will form [Ref. 4, 18, 19, 21]. Figure 5 depicts typical
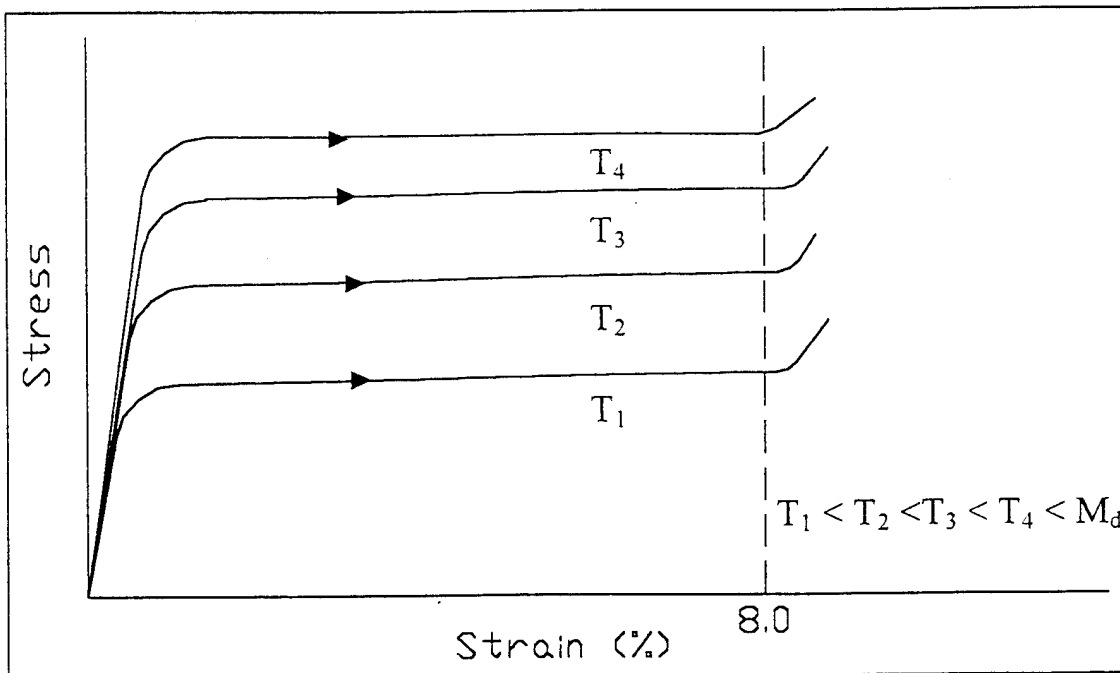

T4

T3

T2

T1

$T_1 < T_2 < T_3 < T_4 < M_d$

Strain (%)   8.0

Stress

Figure 5. Loading stress-strain curves of a Superelastic Alloy at various temperatures between A_f and M_d.

loading stress-strain curves for a Superelastic Alloy over a range of temperatures in the superelastic range.

B. ADVANTAGES OF SUPERELASTIC ALLOY

The stress-strain relationship shown in Figure 5 reveals that as the temperature is increased, an SEA element can withstand greater stresses without reaching the loading

stress plateau and superelastic strain. By use of the Clausius-Clapeyron equation, the amount of force required to reach the loading stress plateau for a certain temperature can be accurately predicted [Ref. 4, 18]. An SMA element does not exhibit this property. An example of this is seen in Ni-Ti tubes manufactured by Raychem corporation. Superelastic Alloy (composition Ni-50.0 at. % Ti) and Shape Memory Alloy (composition Ni-49.2 at % Ti) tubes of similar dimensions were subjected to three point bending tests and the results were compared. At 23°C, the SEA tube has a loading stress of approximately 450 MPa. When the temperature of the SEA tube was increased to 37°C the loading stress increased to approximately 550 MPa. As the temperature was increased, the loading stress increased at a rate of approximately 7 MPa/ °C [Ref. 4]. An incremental change in the temperature of the SEA will result in a proportional change in the loading stress. In comparison, the Raychem SMA tube does not have a loading stress that varies with temperature. Below A_f, an SMA is in a martensitic phase. Twin boundaries will migrate if any force is applied to the tube, resulting in large strain but little stress. If the SMA tube is heated above A_f, the resulting phase transformation from martensite to austenite will create an SMA martensite plateau stress [Ref. 4]. The Raychem SMA tube has a martensitic plateau stress of only 138 MPa. This stress is only realized if the tube is heated to the A_f of 50°C [Ref. 4]. The martensite plateau stress found in SMA cannot be incrementally changed with temperature. The only way to change the martensite plateau stress is to cool the SMA tube to below M_f. This facilitates the phase transformation of austenite back to martensite, eliminating the martensite plateau stress.

SEA can endure strain up to 8.0% without "amnesia" or plastic deformation [Ref. 19]. As shown in Figure 5, at the onset of strain, the SEA exhibits Hookean properties with a very large modulus until σ_l is reached. For an SEA at room temperature, the strain associated with the onset of the loading stress is approximately 1.5% [Ref. 4]. This large allowable strain margin of 6.5% only decreases by approximately 0.75% over a 60°C temperature range between A_f and M_d [Ref. 19].

An SEA can also regulate the amount of internal stress as the actuator is deformed. If the actuator is subject to a deformation, the growth of martensite will occur as is the σ_l plateau is reached. The growth of SIM will regulate the maximum internal stresses, accommodating the strain as it increases but never allowing it to exceed the value of σ_l for the particular temperature. If the stress increases somewhere in the element, SIM will grow and maintain the loading stress as long as the maximum strain is not exceeded.

C. CYCLE FATIGUE OF SUPERELASTIC ALLOY

Cyclic loading of Ni-Ti alloys can result in the loss of superelastic properties. It has been shown that when stresses are cyclically applied, Ni-Ti alloy will show fatigue effects which can reduce the performance of the actuator. Stress cycling fatigue effects include amnesia and a decrease of the loading stress required to induce martensite. Amnesia is the inability of an SEA element to return to its original undeformed shape upon unloading of the cyclic stress [Ref. 24, 25].

Amnesia and the decrease in loading stress is caused by slip deformation in the SEA crystalline structures. Crystal structures permanently shift to accommodate the shear force applied to the lattice during deformation of the SEA element. When the stress is reduced on the specimen, slip deformation remains, leaving both a residual plastic strain in the specimen and residual internal stresses in the crystal structures [Ref. 22, 23, 24]. The residual plastic strain is the amnesia the element encounters upon unloading. The residual internal stresses will assist in the formation of SIM. Less external stress needs to be applied to the specimen to reach the critical stress necessary to promote SIM growth. Therefore, the magnitude of the loading stress actually decreases.

Investigation of the effects of cyclic stress has revealed amnesia and loading stress reach constant values over an increasing number of cycles [Ref. 25]. This is due to a finite number of dislocations found in the crystal structure of the alloy. As the specimen is cycled, the number of dislocations available for the accommodation of slip decreases. This results in an initial increase of the amnesia which reaches a maximum after a finite number

of cycles. Of the two adverse effects of cyclic loading, amnesia is the most detrimental to the performance of the actuator. The residual plastic strain associated with amnesia reduces the actuator's effective displacement. A solution is therefore necessary to prevent cyclic stress effects.

Reduction of cyclic stress effects ensures reliable motion of the actuator by stabilizing the superelastic characteristics of the alloy elements. Since cyclic stress effects are the result of slip, it is necessary to raise the critical stress required to induce slip to a value above the loading stress of the actuator SEA element. This can be accomplished by thermal-mechanical treatment of the alloy. The most effective method of suppressing slip is introducing dislocations by cold working the alloy and then thermally rearranging them to achieve an evenly dispersed dislocation density. It has been shown that an optimum annealing temperature for near equiatomic Ni-Ti alloy is around 400°C [Ref. 25]. Annealing temperatures above 400°C will result in the annihilation of dislocations through re-crystallization and grain growth. Changes in the crystalline structures can also result in an elevation of A_f, or a decrease in the value of σ_l.[Ref. 22, 25]. Due to these drawbacks, caution must be exercised in the annealing of Superelastic Alloys to ensure the annealing temperature is not above 400°C.

D. RESISTANCE CHARACTERISTICS OF SEA AT ELEVATED TEMPERATURES BELOW M_d

Most research on SEA has been centered around its characteristics near A_f. Our concern is how Superelastic Alloy behaves over the entire temperature range from A_f to M_d. Miyazaki performed electrical resistance measurements over a temperature range from below M_f to M_d in his research of cycling effects on superelastic Ni-Ti alloys [Ref. 25]. During the heating of the Superelastic Alloy below A_f, his plots show that SEA has a resistance trend similar to the plot depicted in Figure 2. Above A_f, the resistance peaks, drops a little and then plateaus at a constant value. The plateau occurs approximately 20°C past A_f and remains to M_d. Figure 6 is an approximate reproduction of the trend

Miyazaki's plots followed during the heating portion of his experiments. A search of relevant technical literature did not produce an explanation for this sudden drop in electrical resistance. Similar drops in electrical resistance are evident during phase transformations in Shape Memory Alloys. However, in Superelastic Alloy at temperatures above A_f there is no phase transformation when no external stress is applied. The results of Miyazaki indicate the phenomena associated with the change in resistance occurs in all Ni-Ti Superelastic Alloys and is repeatable over a large number of cycles. Therefore,
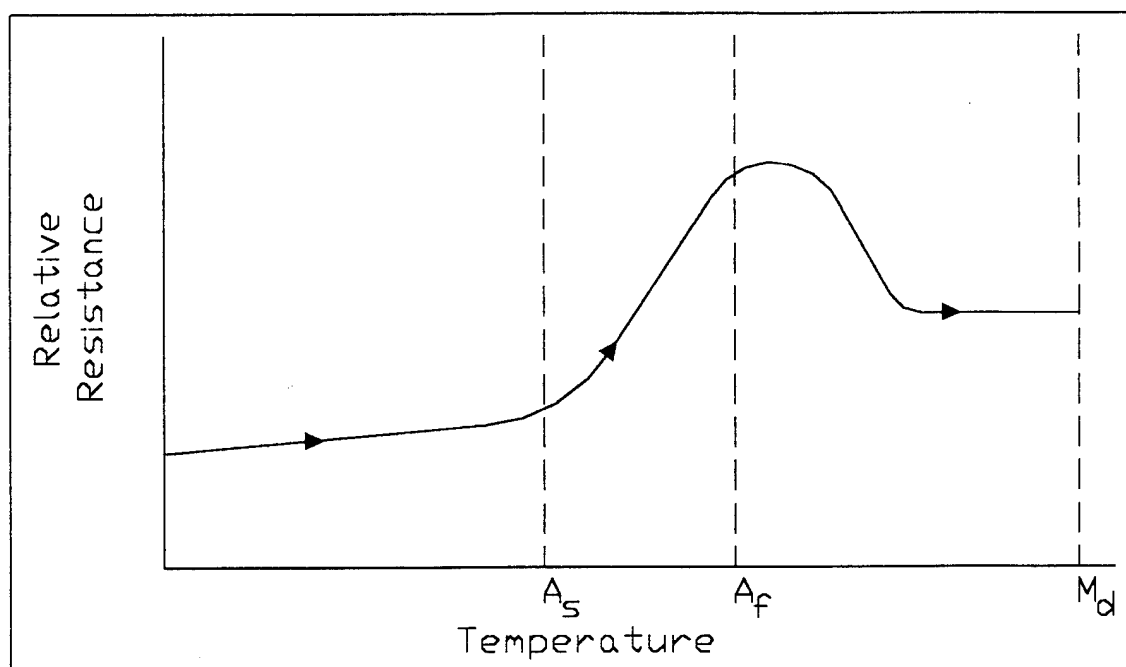

Figure 6. Relative resistance trend of a Superelastic Alloy vs. temperature [Ref. 25].

without trying to present an explanation, it is our intent to utilize this phenomena in the designing of a feedback control law for the SEA actuator element. This will be explained in the next chapter.

Our experiments were conducted on a Raychem type BB alloy tube of dimensions: 1.129 mm O. D., 0.978 mm I. D., and 40.0 mm length. The first experiment was a very basic bench test of the dependence of the loading stress on temperature. A Raychem tube

was connected to a current source and placed across a simple support with a weight of approximately 1.0 pound suspended from its ends so the tube bent downward over the support at room temperature as shown in Figure 7. Almost as soon as the electrical current was started, the tube straightened to almost its original unbent shape. Only the residual strain due to the presence of the 1 pound weight remained.

For the next experiments the Raychem type BB alloy tube was annealed at 475°C for 25 minutes while constrained by a 4.0 cm radius circular jig to impart a curved shape.
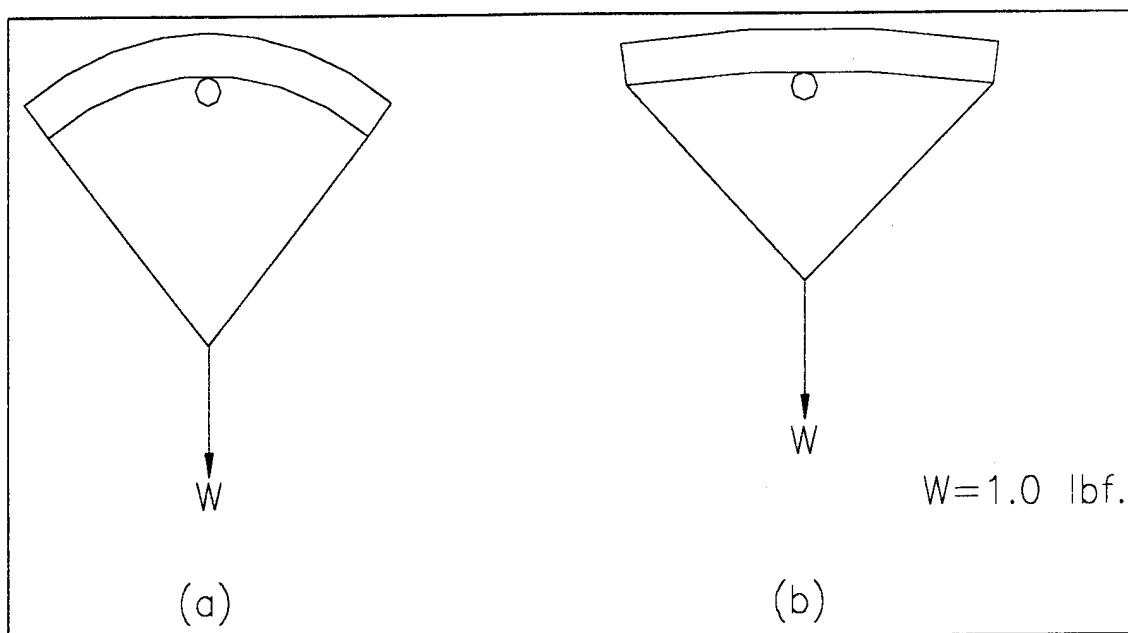

Figure 7. (a) Raychem tube bench test with no electrical current. (b) Same tube with 3.0 amps of electrical current.

The A_f of the BB alloy is reported to be 5.0°C by Raychem, but this value was raised by our annealing process. The annealing at elevated temperatures has the adverse effect of raising the value depending on time and temperature annealed [Ref. 4, 21, 25]. The tube was placed in the apparatus shown in Figure 8 were weights were hung from the center to impart a strain on the tube. The tube was lowered into a temperature bath where the resistance was measured using a Hewlett-Packard 34566A Digital Multimeter in a four

wire resistance measurement configuration. Three experiments were conducted with no weight, 1.0 pound, and 1.25 pound weights hanging from the tube. The weights are approximate since they were suspended in the temperature bath with the SEA tube and no compensation was made for buoyancy effects. Figures 9, 10 and 11 are plots of the experimental results.
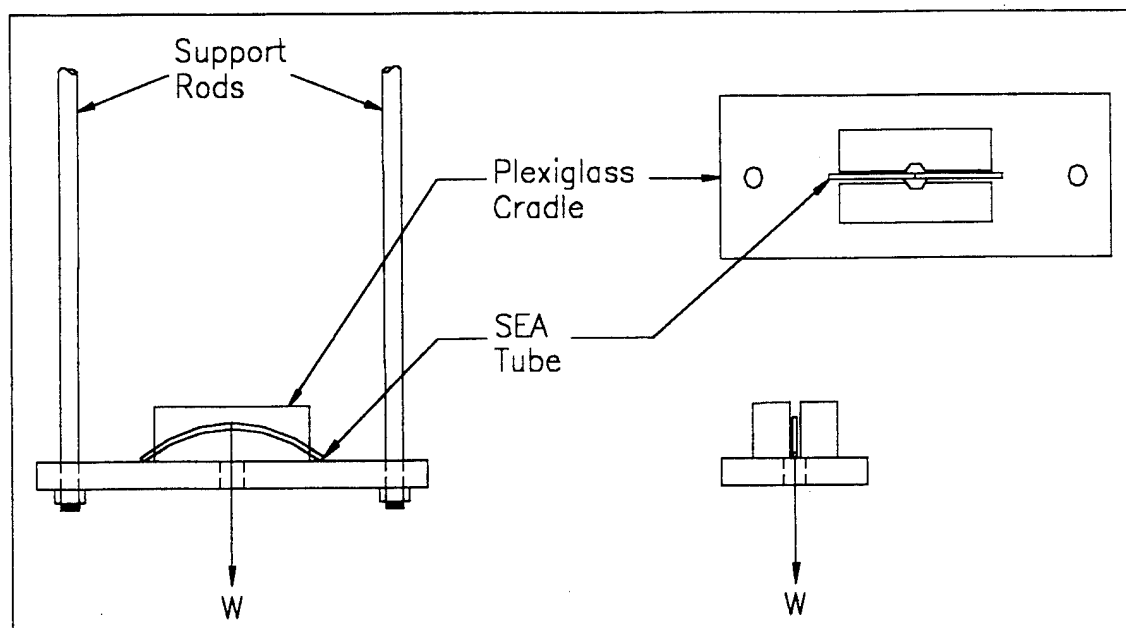

Figure 8. Plexiglass cradle used for immersing Raychem SEA tube in temperature bath.

A comparison of these experimental results to the those obtained by Miyazaki [Ref. 25], support two conclusions. Even with the additional annealing process we used to impart the curved shape on the tube, the A_f temperature was found to be between the original 5.0°C, the initial A_f temperature provided by Raychem, and 17.7°C, the lowest temperature investigated for our current experiment. Therefore, for our applications above room temperature, the Ni-Ti alloy will remain superelastic. Additionally, the experimental results show that over the temperature range tested, the resistance plots start
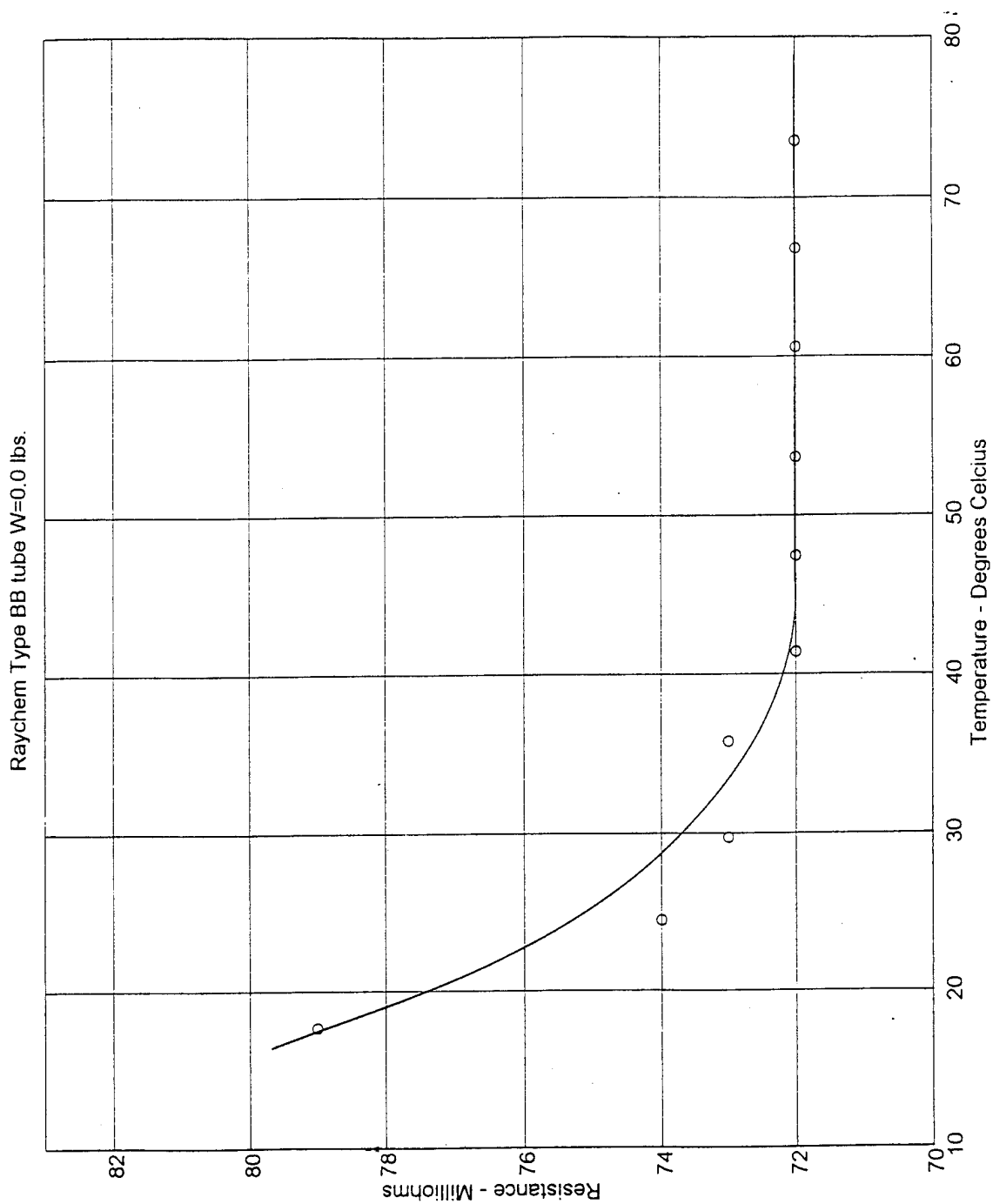
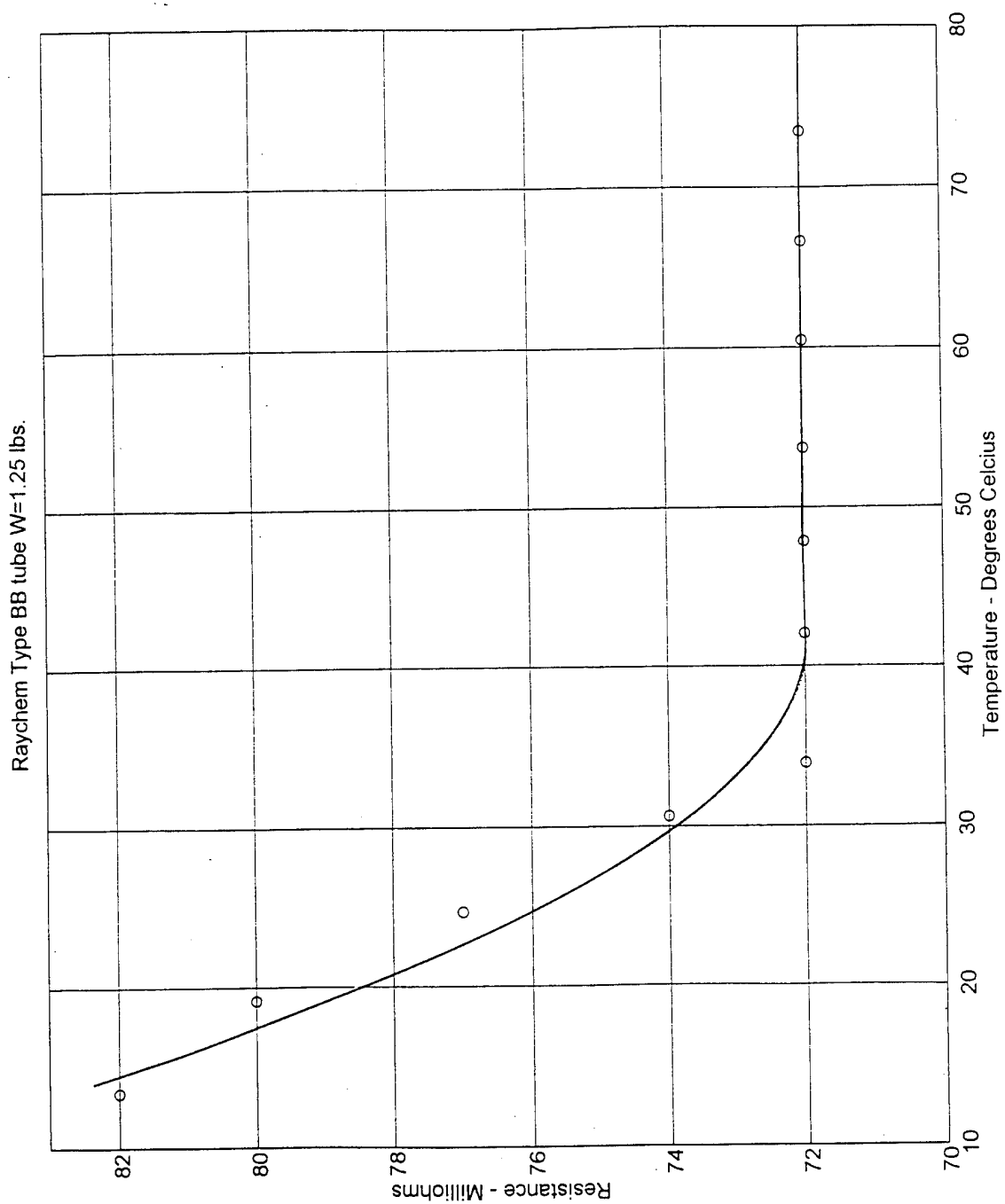**Figure 9.** Experimental plot of resistance vs. Temperature for SEA tube, W = 0.0 lbs.

20

Figure 10. Experimental plot of resistance vs. Temperature for SEA tube, W = 1.25 lbs.
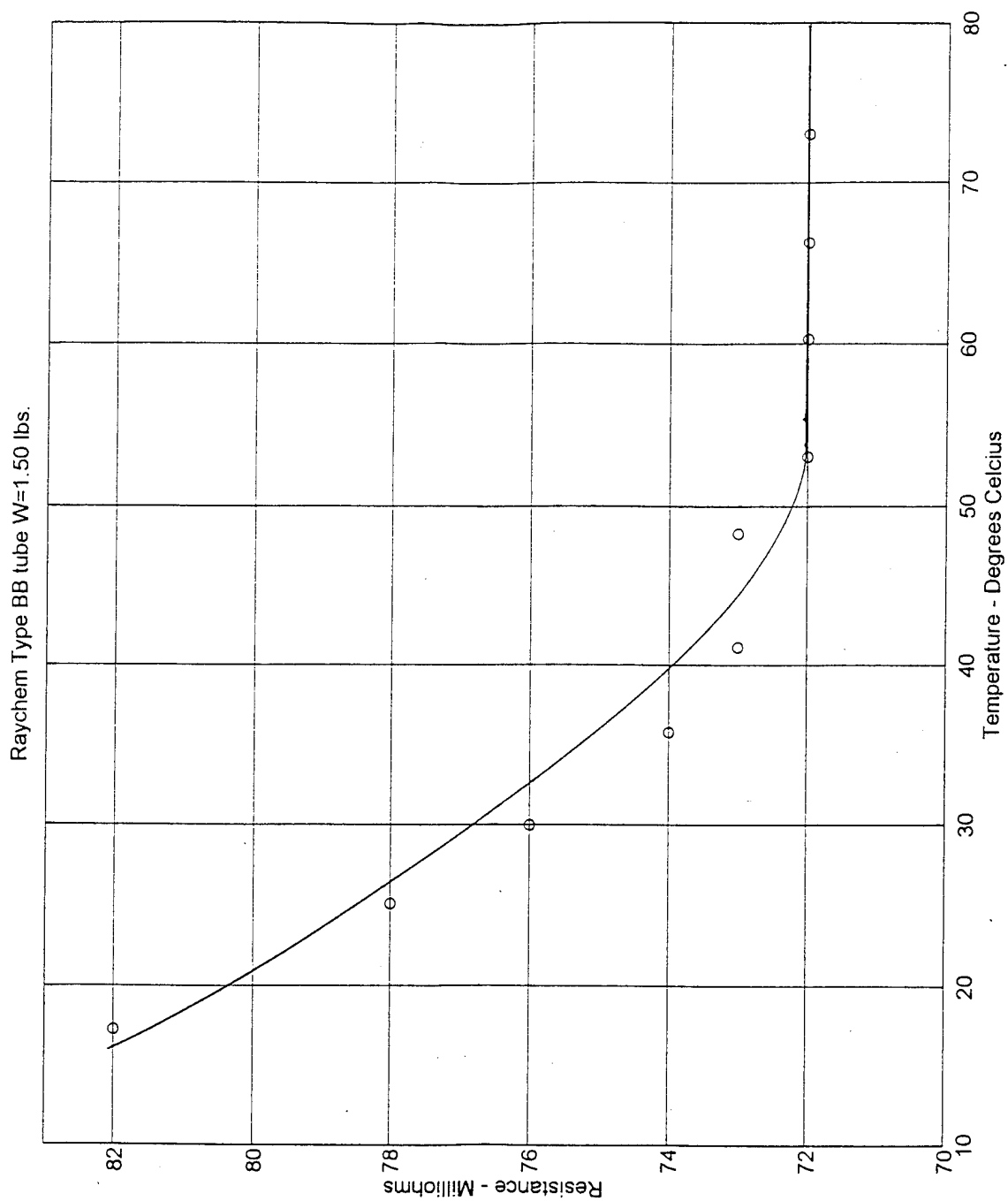
Figure 11. Experimental plot of resistance vs. Temperature for SEA tube, W = 1.5 lbs.

at a point past the A_f resistance peak, decreases and finally reach the resistance plateau approximately 20-30°C above room temperature. The resistance decreased at approximately 0.73 mΩ/°C with no weight, 0.63 mΩ/°C with 1.0 pound, and 0.51 mΩ/°C with 1.25 pounds attached. The plateau resistance for all runs was 71-72 mΩ. A second phenomena is apparent in these experimental plots. As the weight hanging from the tube is increased, there is a shift of the resistance curve upward. This is contradicting to the current technical research. When a stress is applied to the SEA tube, the growth in martensite should result in an inherently lower resistance than the tube with no stress applied. As the tube is heated, the subsequent heating of the alloy and the phase transformation back to austenite should result in an increase in resistance [Ref. 18]. The SEA apparently contradicts the expected results and a search of technical literature found no explanation for this occurrence. Regardless, this topic is beyond the scope of this thesis and the resistance drop will be used as a means of feedback control.

As supported by both our experiments and Miyazaki's results, the *relative* resistance trend for Ni-Ti superelastic tube is a repeatable occurrence. Therefore, it is our conclusion that regardless of the number of cycles the Ni-Ti Superelastic Alloy endures or its physical dimensions, the same resistance *trend* exists at temperatures between A_f and M_d.

IV. THE CONCEPT BEHIND THE SEA ACTUATOR

A. SEA RESPONSE TO TEMPERATURE VARIATIONS

It was discussed in Chapter III that the loading stress of a Superelastic Alloy is a function of temperature. If the internal stress equals the loading stress for a specific temperature, Stress Induced Martensite will grow in the element and a corresponding
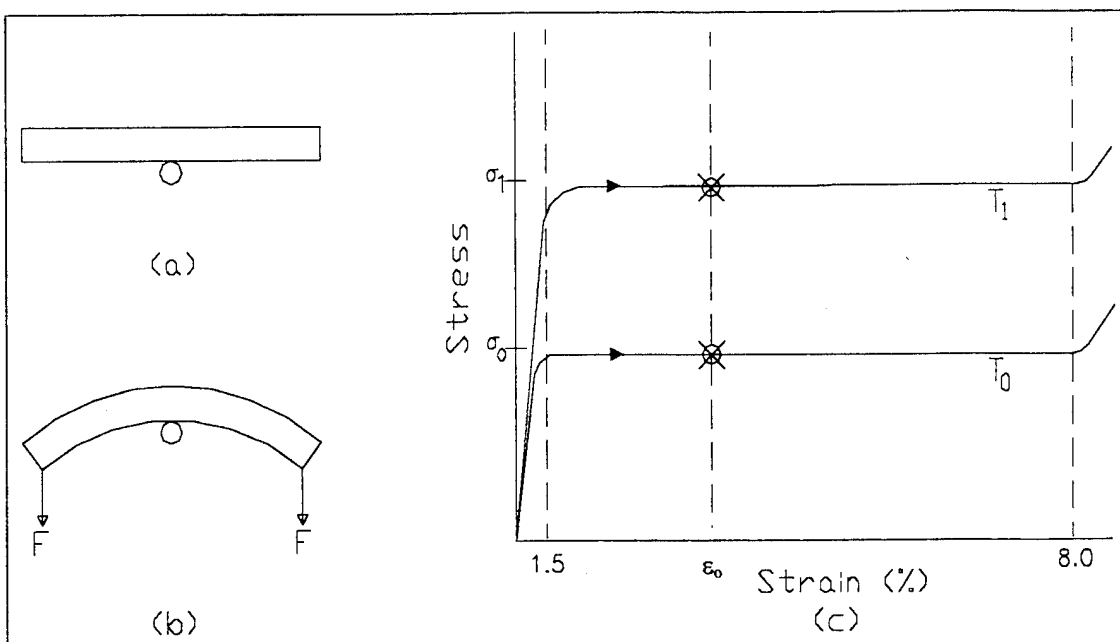
Figure 12. (a) , (b) Example of an SEA element under increasing end loading. (c) Corresponding stress-strain curve, $T_1 > T_0$.

strain will develop in the element. An increase in the temperature of the SEA element will increase the loading stress plateau. The higher loading stress will force a phase transformation of the Stress Induced Martensite back to austenite. This transformation results in the elimination of some or all of the strain in the SEA element. The temperature dependency of SEA loading stress makes it possible to use the SEA element

for applying actuation forces. Figures 12 and 13 are used to help explain this concept of applying actuation forces by changing the element temperature.

In Figure 12(a), an SEA element is placed across a simple support at temperature T_o such that $A_f < T_o < M_d$. A force F is applied on each end and increased until the element has a certain amount of strain ε_o, as shown in Figure 12(b). At this point, the maximum stress is equal to the loading stress σ_0, corresponding to temperature T_o. If the overall strain does not exceed 8.0%, the element will exhibit full superelasticity and
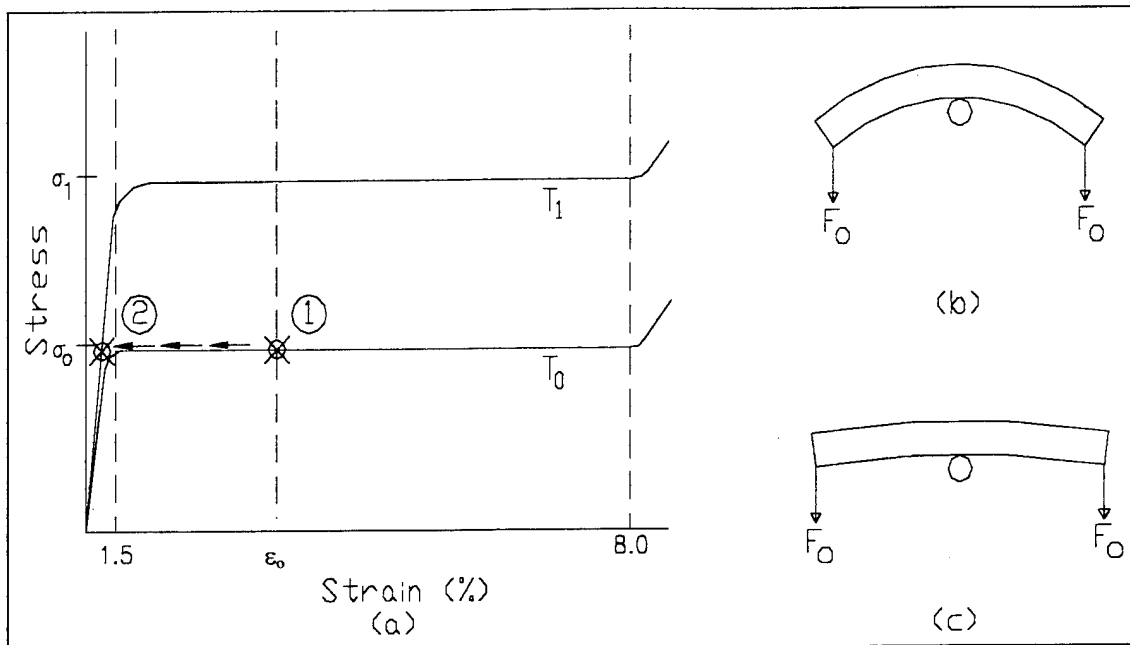

Figure 13. (a) Stress-strain curve of SEA element, $T_1 > T_o$. (b) SEA element at T_o with force F_o applied to ends. (c) SEA element at T_1 with force F_o applied to ends.

recover its original shape upon unloading of the force. The stress-strain curve for this deformation is shown in Figure 12(c). The point marked on the stress-strain curve at temperature T_o represents ε_o strain in the element for the corresponding loading stress σ_0. Using the same procedure of applying the force F to the ends of the element, the element temperature is raised to $T_o < T_1 < M_d$. The force F, is applied to the ends and increased gradually until the element reaches the same strain ε_o. The stress-strain curve for

26

temperature T_1 in Figure 12(c) reveals that at the elevated temperature, the loading stress increases to σ_1. A greater force must be exerted on the element ends before the particular strain ε_o can be reached. The point marked on the stress-strain curve at temperature T_1 represents ε_o strain in the element for the loading stress σ_1.

The procedure is varied slightly as depicted in Figure 13. At T_o, a constant force F_o is applied to the ends of the element. F_o is great enough to reach the loading stress σ_o and the strain ε_o. In Figure 13(a), point ① is the position on the stress-strain curve for this condition and Figure 13(b) illustrates the deformed SEA element. Keeping F_o constant, the temperature of the element is increased to T_1. When the temperature of the element is raised, the critical stress for the element is raised from σ_0 to σ_1. This increase will result in unstable SIM transforming into the austenite parent phase, and the alloy will not be able to maintain the strain ε_o. The phase transformation of SIM to austenite forces the element back to its pre-strained shape. In Figure 13(a), point ② is the position on the stress-strain curve for the increased temperature T_1. Since F_o is still applied to the element, a small amount of residual elastic strain (between 0.5 to 1.5%) is present. With the exception of the residual strain, the element will recover to its pre-strained shape at T_1 as depicted in Figure 13(c). If the element is cooled to T_o, the austenite will transform back into SIM since the loading stress is reduced to σ_o. The result will be the SEA element bending under the applied force F_o to strain ε_o. The effect of the temperature decrease from T_1 to T_o is also illustrated on the stress-strain curve of Figure 13(a), where the element will translate from point ② back to point ①.

This illustrates the concept of actuation. If the temperature of an SEA element is increased from T_o to T_1, the active element can produce a displacement in the presence of an external force F_o. The displacement is due to the phase transformation of SIM to austenite associated with the increase of temperature and can be maintained if the element is kept at the corresponding high temperature. The displacement in the presence of the external force F_o is removed in the element when it is returned to the lower temperature. This is the concept which will be used in our actuator design.

B. THE SEA ACTUATOR

The relative merits of a Superelastic Alloy over a Shape Memory Alloy, presented in the previous chapter and section, have influenced our decision to use an SEA active element as part of our actuator design. Specifically, an SEA tube has been chosen for the active element. There are two reasons a tube has been chosen in our design. First, Ni-Ti SEA tubes are manufactured by several companies who offer a variety of dimensions and austenitic finish temperatures. Second, a tube is easier to heat by electrical current due to its reduced cross-sectional area. Compared to a solid element of similar outer diameter, there is a significant reduction of the cross-sectional area from that of a solid rod of equal outer diameter. This smaller cross-sectional area greatly increases the electrical resistance of the actuator compared to a solid rod, or other element of similar cross-sectional area. Therefore, a reduced electrical current is needed for heating the actuator to the proper actuating temperature. The area moment of inertia is also reduced, which proportionally reduces the SEA tube strength. Although the area moment of inertia is reduced, there is still sufficient operating strength for application in our actuator design with a Ni-Ti Superelastic Alloy tube.

The SEA element chosen for our actuator design is fabricated from a Raychem type BB Ni-Ti alloy tube. The tube has an outside diameter of 1.129 mm, an inside diameter of 0.978 mm, and an overall length of 31.0 cm. The estimated austenitic finish temperature (A_f) for the Ni-Ti Superelastic Alloy is 5.0°C. Three 45 mm elements are cut from the tube stock. The tubes are constrained using a circular stainless steel jig and annealed at 475°C for 25 minutes. The constrained annealing imparts a curved shape on the tubes so that they can be used as the active elements in the actuator.

The curved SEA tubes are fixed in a metallic disk as illustrated in Figure 14(a). The tubes are spaced 120° around the central axis of the disk. Each annealed tube faces radially outward from the central axis of the metallic disk. The metallic disk has an outside diameter of 10.0 mm and a thickness of 5.0 mm. The SEA tubes are soldered into the metallic disk. Two non-metallic disks, constructed of Delrin, pass over the curved SEA tubes and constrain them in the position illustrated in Figure 14(b). The Delrin disks
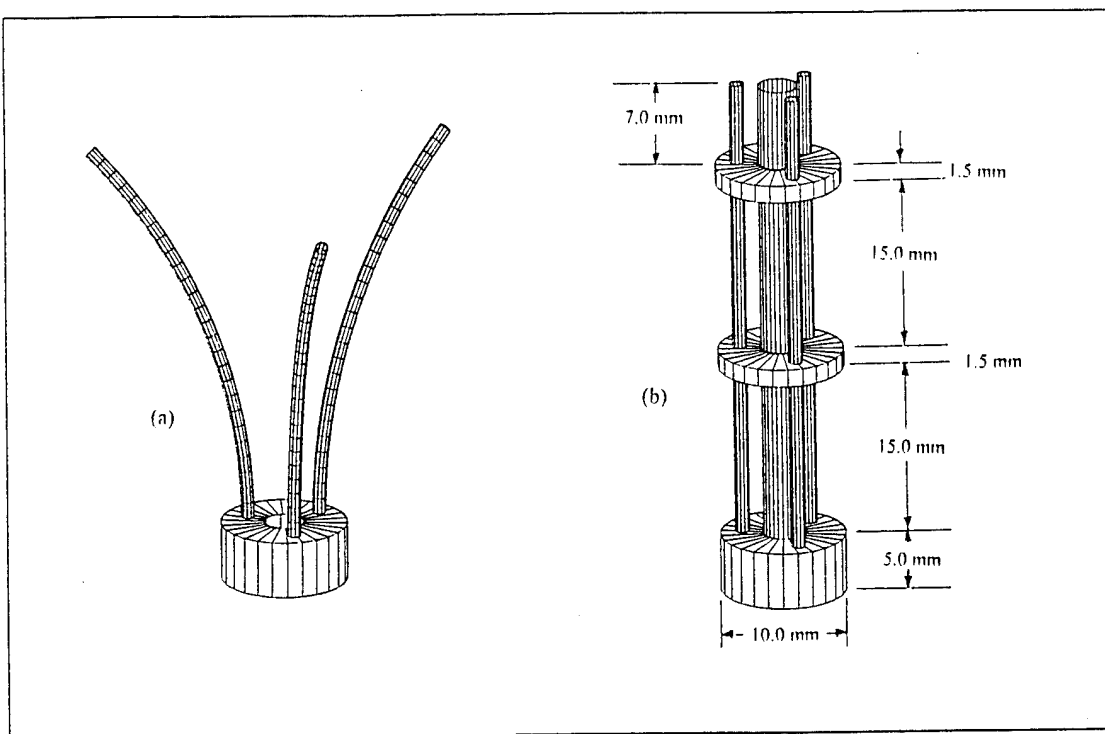

Figure 14. (a) The annealed SEA tubes fixed to the metallic disk base face radially outward. (b) The annealed SEA tubes fixed to the metallic disk base are constrained by the two Delrin disks. Also depicted is the nylon annular tube passing through the actuator.

have an outside diameter of 10.0 mm, and a thickness of 1.5 mm. The spacing between each disk is 15.0 mm. The SEA tubes extend 7.0 mm beyond the top Delrin disk, which allows them to bend without slipping out of the top disk. The diameter of the holes in the Delrin disks which constrain the SEA tubes is 1.20 mm. This is slightly larger than the

29

outside diameter of the SEA tubes to allow for the movement of the tube. Delrin, a material similar to Teflon, has been chosen because of its electrical insulative properties, high tensile stress, hardness, melting temperature of 170°C, and low coefficient of friction. The low coefficient of friction will assist in the movement of the tubes as they slide through the disks.
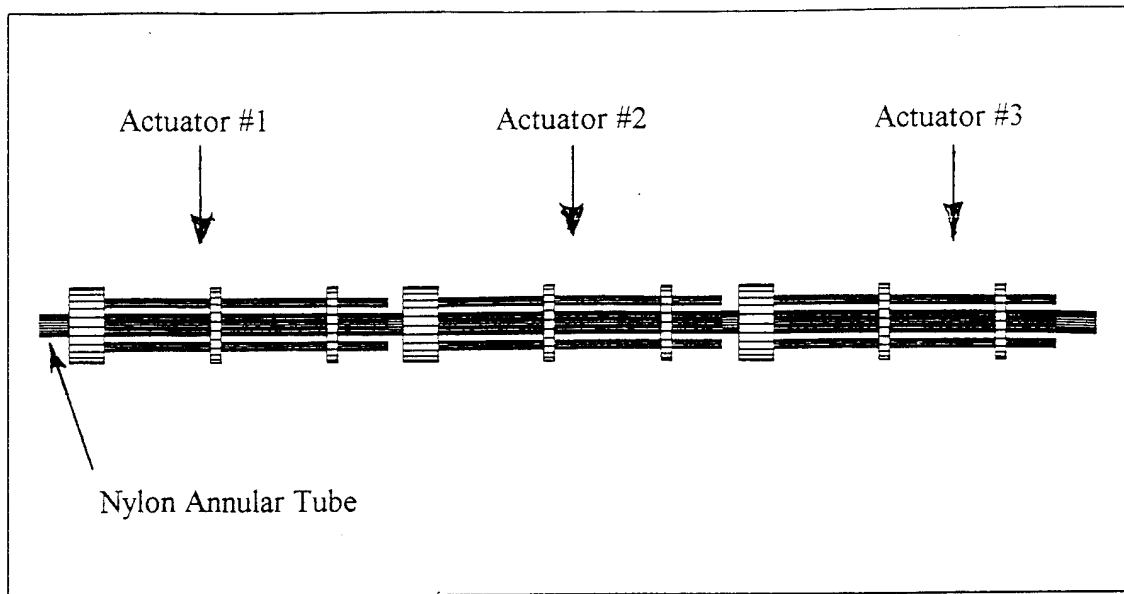

Figure 15. The configuration of three SEA actuators along the annular nylon tube. Each actuator disk is fixed to the annular nylon tube.

Figure 15 illustrates how a series of three actuators are connected. The metallic and Delrin disks in each individual actuator contain an axial hole. A single annular nylon tube passes through these holes, and is fixed to each disk thus binding the actuators. The nylon tube has an outside diameter of 3.5 mm, and was chosen because of its stiffness and resistance to being crushed or kinked. The nylon also has a high ultimate tensile stress and melting temperature of 110°C.

Figure 16 illustrates the operation of the actuator. The three basic directions the tip of the actuator can move, labeled R_1, R_2, and R_3, are located 120° apart radiating outward from the center of the metallic disk. The Delrin disks force the SEA tubes into a straight position, inducing a strain of approximately 4.5% and an internal stress equal to the loading stress necessary for superelasticity. This resulting force places the elements in an antagonistic situation, where they equally oppose one another when at the same
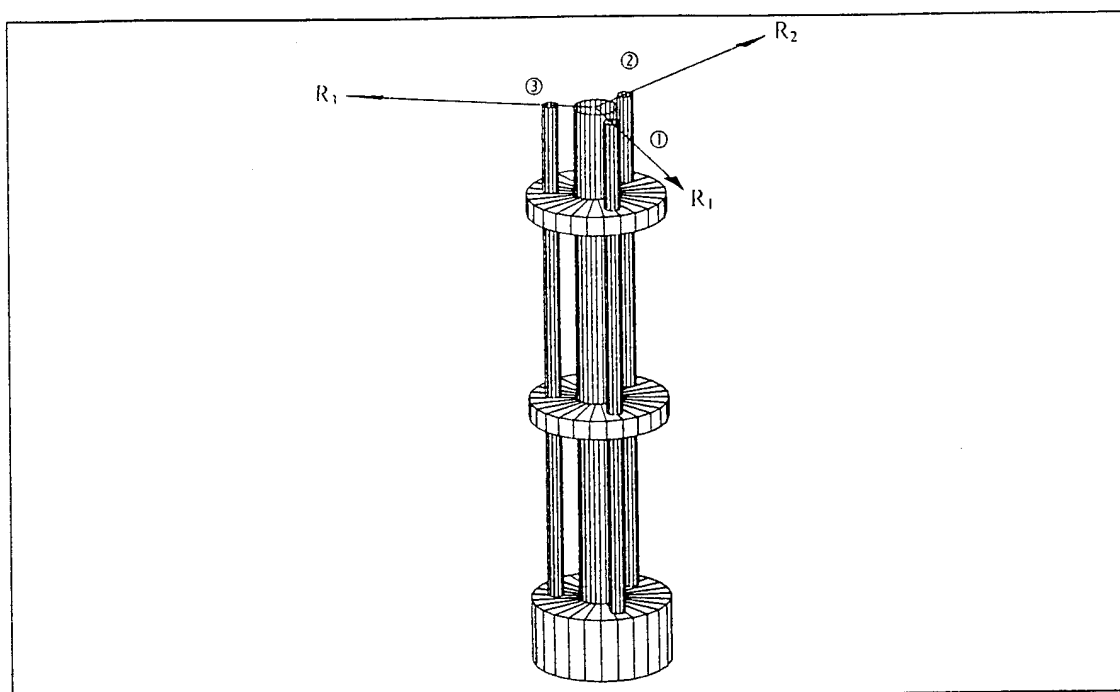

Figure 16. The SEA actuator. The SEA tubes, ①, ②, ③, the metallic base disk, the two Delrin disks, and the annular nylon tube. The annular tube will pass through the entire length of the manipulator. The three corresponding directions of movement are R_1, R_2, and R_3.

temperature. The SEA tubes are connected to an electrical current source. The metallic disk is used as a common connection and each free SEA tube end is connected to a multiple throw switch. To move the actuator in the R_1 direction, tube ① is heated by electrical current. This increase in temperature raises the loading stress in tube ① and the SIM will undergo a phase transformation to austenite. Tube ① will move in the presence

of the antagonistic forces of the other two SEA tubes from the straight position to its original curved, annealed shape. The other two SEA tubes will have a lower loading stress and are not able to resist the force generated by tube ①. The actuator will move in the R_1 direction. The strain in tube ① will go from 4.5% to the threshold strain of 0.75-1.5% strain. The maximum strain the passive tubes ② and ③ will endure when tube ① is heated is 7.5%; the 4.5% strain induced when they are forced from a curved to a straight shape by the Delrin disks, and 3.0% when tube ① bends them back further. The actuator will maintain this position in the R_1 direction as long as the temperature in the active tube is higher than the passive ones. The actuator can be bent in any of the three directions by heating the perspective single SEA tube or can be bent by the heating of any combination of two SEA tubes.

C. MERITS OF THE SEA ACTUATOR

The characteristics of the SEA actuator make it a far more suitable choice for our purposes over conventional SMA actuator designs [Ref. 2, 3, 7, 9]. In this section we will discuss the minimization of cooling rate problems, the ability of SEA's to regulate internal stresses, and how the resistance characteristics at elevated temperature below M_d make a Superelastic Alloy tube an ideal element for a feedback control system.

The heating rate of the SEA tube is directly proportional to the magnitude of the electrical current while the cooling rate is related to the heat capacity of the alloy and the surface area of the tube. Due to the size constraints of the actuator, increasing the surface area of the SEA tube is not feasible, and the heat capacity of Ni-Ti is difficult to modify. Since the SEA tubes heat up many times faster than they cool down, the actuating current can be modified to minimize the effect of the slow cooling rate. This is accomplished by introducing an actuating current which creates a specific temperature profile in the SEA tube. Referring to Figure 16, if the actuator is bent in the R_1 direction, SEA tube ① has an operating current I_{op} passing through it which heats it to an operating temperature T_{op}. If it is desired to move the actuator to the R_2 direction, the current is switched off in tube

①, which begins to cool. The current in tube ② is simultaneously turned on, but to a higher current, $I > I_{op}$. This will heat tube ② to a $T > T_{op}$. Almost immediately there is a temperature difference between tubes ① and ② that is great enough to move the actuator from the R_1 direction to the R_2 direction without waiting for tube ① to cool. After a period of time, the current and temperature can be reduced in element ② to the operating levels, I_{op} and T_{op}, and another movement can be induced on the actuator.

The ability of the SEA to regulate the internal stresses in the actuator tube is through the growth of Stressed Induced Martensite. When the SEA tube is strained in the actuator by the Delrin disks, the internal stress will be equal to the loading stress for the particular temperature of the tube. If the passive SEA tube is bent further by an active one, the strain in the passive tube increases to the maximum design strain of 7.5%. As the strain increases, the internal stresses of the tube never exceeds the plateau loading stress due to the growth of SIM. An incremental increase of the internal stress above the loading stress induces more martensite to grow. The growing martensite undergoes detwinning to accommodate the strain and reduces the internal stress of the SEA tube down to the loading stress value. As long as the strain of the SEA tube does not exceed 8.0%, the stress never exceeds the loading stress. This protects the SEA tubes from permanent deformation and catastrophic stress failure. This mechanism also regulates the internal stresses of the tube when it is active. When heated, an active tube moves against the forces created by the other two SEA tubes. This movement creates an internal stress in the active SEA tube. If an additional external force is exerted on the actuator, for example by an obstruction, it could increase the internal stress of the active tube beyond its capability, resulting in a failure or permanent deformation of the tube. Instead, due to the growth of SIM, the internal stress of the tube does not exceed the loading stress and a safe internal stress is maintained.

The resistance characteristics of SEA between A_f and M_d make feedback control of the actuator possible. It is necessary to monitor and control the temperature of the SEA tubes so they do not exceed M_d. Above M_d the SEA tubes will permanently deform

if strained. By sampling the resistance of the SEA tubes, their temperatures can be accurately predicted. As shown in Figures 9-11, as the temperature increases, the resistance decreases sharply and then plateaus at a constant value, regardless of the internal stresses of the tube. The resistance plateau occurs approximately 20-30°C above room temperature and 40-50° below M_d. This constant resistance plateau begins at the temperature we wish to heat the element for actuation, T_{op}, and makes temperature control through resistance feedback possible. When an electrical current is passed through an SEA tube, the temperature of the tube will increase and the resistance decreases. The resistance is sampled at an appropriate frequency, and the tube is at the correct temperature when there is no longer a change in resistance. With the plateau starting 40-50°C below M_d the chance of overheating and permanently deforming the tubes is greatly reduced. The two electrical currents previously discussed can also be controlled using this system. The higher current, $I > I_{op}$ can be passed through the tube at the start of the heating cycle. When the plateau is reached, the current can remain on for a pre-determined number of sampling cycles to allow the element to reach the temperature $T > T_{op}$, and then be turned off. When the resistance begins to increase as the element cools to below the operating temperature T_{op} the operating current I_{op} is then used to maintain the temperature. This resistance phenomena is ideal for the feedback control of the SEA actuator.

V. SUMMARY AND RECOMMENDATIONS

Our actuator for a minimally invasive surgical manipulator was designed around the use of near equiatomic Nickel-Titanium Superelastic Alloy tubes as the active elements. Since very little research has been completed on these alloys for use as active elements, the most important goal of this research was to investigate whether an SEA element could be a controllable and reliable component in an actuator. We introduced the physical properties and characteristics of SEA's, with an emphasis on the dependence of loading stress on temperature. Two experiments were conducted. In the first experiment we successfully validated the ability of an SEA element to move in the presence of a force when heated to a higher temperature. The second experiment revealed that as the temperature of an SEA element is increased, a repeatable resistance trend exists which can be used in system feedback control of the element temperatures. The concept of applying actuation forces with the SEA tubes by varying of the temperature was then discussed. It was shown that between A_f and M_d, an increase in temperature of an SEA tube could produce a movement of the actuator. Finally, the actuator design was discussed, resulting in a basic concept of the actuator and its integration into the surgical manipulator.

This study has been an initial step in the design of an actuator that will use Nickel-Titanium Superelastic Alloys to control the motion of a minimally invasive surgical manipulator. In the course of future research, a prototype actuator must be developed, and more research is necessary to fully understand the behavior of Superelastic Alloy tubes. More understanding of the relationship between annealing time and A_f would assist in the design of the SEA elements. The SEA element will undergo both temperature and stress cycling. The fatigue life and effect of cyclic loading of Nickel-Titanium Superelastic Alloys must be investigated. The stresses encountered by the SEA tubes under eccentric loading must also be explored. With the unique loading and unloading stresses associated with SEA's, a more in depth understanding of the stress distributions during bending would assist in the determining the optimum design parameters of the SEA tubes.

LIST OF REFERENCES

1. Bergamasco, M., F. Salsedo, and P. Dario, "A linear SMA Motor as Direct-Drive Robotic Actuator," *IEEE International Conference on Robotics and Automation*, pp. 618-623, 1989.

2. Kuribayashi, Katsutoshi, "Millimeter Joint Actuator Using a Shape Memory Alloy," *Sensors and Actuators*, vol. 20, pp. 57-64, 1989.

3. Kuribayashi, Katsutoshi, "A New Actuator of a Joint Mechanism Using Ti-Ni Alloy Wire," *The International Journal of Robotics Research*, vol. 4, no. 4, pp. 47-58, 1986.

4. Proft, J.L., J.W. Simpson, J.A. DiCello, and M.J. Bower, "Superelastic and Shape Memory Nickel-Titanium Microtubing," Technical report, Raychem Corporation, Menlo Park, CA.

5. Furuya, Y., and H. Shimada, "Shape Memory Actuators for Robotic Applications," *Engineering Aspects of Shape Memory Alloys*, pp. 338-355, Ed. T.W. Duerig, K.N. Melton, D. Stöckel, and C.M. Wayman, Butterworth - Heinemann, Boston, MA, 1990.

6. Hunter, Ian W., S. LaFontiane, J.M. Hollerbach, and P.J. Hunter, "Fast Reversible NiTi Fibers For Use In Microrobotics," *IEEE Workshop of Microelectro Mechanical Systems*, pp. 166-170, 1991.

7. Ikuta, K., M. Tsukamoto, and S. Hirose, "Shape Memory Alloy Servo Actuator System with Electric Resistance Feedback for Application for Active Endoscope," *Proc. IEEE International Conference on Robotics and Automation*, pp. 427-430, 1988.

8. Bergamasco, M., F. Salsedo, and P. Dario, "Shape Memory Alloy Micromotors for Direct-Drive Actuation of Dexterous Artificial Hands," *Sensors and Actuators*, pp. 115-119, 1989.

9. Fukuda, T., G. Shuxiang, K. Kosuge, F. Arai, M. Negoro, and K. Nakabayashi, "Micro Active Catheter System with Multi Degrees of Freedom," *IEEE International Conference on Robotics and Automation*, pp. 2290-2295, 1994.

10. Dario, P., R. Valleggi, R. Pardini, and A. Sabatini., "A Miniature Device for Medical Intracavity Intervention," *Proc. IEEE International Conference on Robotics and Automation*, pp. 171-175, 1991.

11. Ikuta, K., M. Tsukamoto, and S. Hirose, "Mathematical Model - Shape Memory Alloy for Designing Micro Actuator," *Proc. IEEE International Conference on Robotics and Automation*, pp. 103-108, 1991.

12. Ikuta, K., H. Fujita, M. Ikeda, and S. Yamashita, "Crystallographic Analysis of TiNi Shape Memory Film for Micro Actuator," *Proc. IEEE International Conference on Robotics and Automation*, pp. 38-39, 1990.

13. Ikuta, K. "Micro/Miniature Shape Memory Alloy Actuator," *Proc. IEEE International Conference on Robotics and Automation*, pp. 2156-2161, 1990.

14. Suzimori, K., S. Iikura, and H. Tanaka, "Development of Flexible Microactuator and its Applications to Robotic Mechanisms," *Proc. IEEE International Conference on Robotics and Automation*, pp. 1622-1627, 1991.

15. Shahinpoor, M., "Electro-Thermo-Mechanics of Resilient Contractile Fiber Bundles as Robotic Actuators," *IEEE International Conference on Robotics and Automation*, pp. 1502-1507, 1994.

16. Ikuta, K., M. Nokata, and S. Aritomi, "Hyper Redundant Active Endoscope for Minimum Invasive Surgery," *Proc. 1st International Symposium on Medical Robotics and Computer Assisted Surgery*, vol. 2, workshop (part I and II), session IV, pp. 230-237, 1994.

17. Neisius, B., P. Dautzenberg, R. Trapp, in cooperation with G. Bueß, "Robotic Manipulator for Endoscopic Handling of Surgical Effectors and Cameras," *Proc. 1st International Symposium on Medical Robotics and Computer Assisted Surgery*, vol. 2, workshop (part I and II), session IV, pp. 238-244, 1994.

18. Weyman, C.M., and T.W. Duerig, "An Introduction to Martensite and Shape Memory," *Engineering Aspects of Shape Memory Alloys*, pp. 3-20, Ed. T.W. Duerig, K.N. Melton, D. Stöckel, and C.M. Wayman, Butterworth - Heinemann, Boston, MA, 1990.

19. Duerig, T.W., and R. Zadno, "An Engineer's Perspective of Pseudoelasticity," *Engineering Aspects of Shape Memory Alloys*, pp. 369-393, Ed. T.W. Duerig, K.N. Melton, D. Stöckel, and C.M. Wayman, Butterworth - Heinemann, Boston, MA, 1990.

20. Funakubo, Hiroyasu, ed., *Precision Machinery and Robotics, Vol. 1 - Shape Memory Alloys*, Gordon and Breach Science Publishers, New York, 1987.

21. Melton, K.N., "Ni-Ti Based Shape Memory Alloys," *Engineering Aspects of Shape Memory Alloys*, pp. 21-35, Ed. T.W. Duerig, K.N. Melton, D. Stöckel, and C.M. Wayman, Butterworth - Heinemann, Boston, MA, 1990.

22. Callister, W.D., *Material Science and Engineering: An Introduction*, 2nd ed., pp. 155-168, J. Wiley and Sons, Inc., New York, 1991.

23. Wood, W.A., *The Study of Metal Structures and their Mechanical Properties*, pp. 93-108, Pergamon Press, New York, 1971.

24. Melton, K.N., and O. Mercier, "The Mechanical Properties of NiTi-Based Shape Memory Alloys," *Acta Metallurgica*, vol. 29, pp. 393-397, 1981.

25. Miyazaki, S., "Thermal and Stress Cycling Effects and Fatigue Properties of Ni-Ti Alloys," *Engineering Aspects of Shape Memory Alloys*, pp. 395-413, Ed. T.W. Duerig, K.N. Melton, D. Stöckel, and C.M. Wayman, Butterworth - Heinemann, Boston, MA, 1990.

INITIAL DISTRIBUTION LIST

1. Defense Technical Information Center   2
    Cameron Station
    Alexandria, Virginia, 22304 - 6145

2. Library, Code 52   2
    Naval Postgraduate School
    Monterey, California, 93943-5101

3. Department Chairman, Code ME   2
    Department of Mechanical Engineering
    Naval Postgraduate School
    Monterey, California, 93942-5000

4. Professor R. Mukherjee, Code ME/MK   3
    Department of Mechanical Engineering
    Naval Postgraduate School
    Monterey, California, 93942-5000

5. Curricular Officer, code 34   1
    Department of Mechanical Engineering
    Naval Postgraduate School
    Monterey, California, 93942-5000

6. LT William T. Parkhurst II   2
    600 West Sixth Street
    Madera, California, 93637